

Application of Image Analysis to Establish Potential Relationship between Intracellular Interaction and Cell Migration Behavior

Tanvir Ahmed^{1,2}, Muhammad Shafiqul Munir² and Shoeb Ahmed^{3,*}

¹Department of Applied Chemistry and Chemical Engineering, University of Dhaka, Dhaka, Bangladesh

²Department of Chemical Engineering, Bangladesh University of Engineering and Technology, Dhaka, Bangladesh

³Department of Chemical Engineering, Bangladesh University of Engineering and Technology, Dhaka, Bangladesh

*E-mail: shoebahmed@che.buet.ac.bd

Received on 29 November 2021, Accepted for publication on 28 July 2022

ABSTRACT

In order to predict the movement and behavior of important cellular components computational language-based image processing approach caters a lot more than the traditional approaches. In this study, a relation of PI3K protein activity during cell migration has been evaluated using MATLAB based custom coding as an image analysis tool. Cells were imaged under fluorescence microscope to detect the PI3-Kinase activity in tandem with the morphological changes. Several cell movement metrics were assessed, indicating protein activity localization. Different parametric analysis confirms that cell migration is essentially controlled by the peripheral activity rather than the overall cell activity. A quantitative relationship has been proposed as a function of high intensity region area, intensity, and angle of movement, which fit 85% of total cellular responses. Customized analysis at intracellular cellular level has the potential to reveal some fine detail that eventually could contribute to the research on the critical diseases like cancer.

Keywords: cell signalling; cell activity; MATLAB; PI3-Kinase

1. Introduction

Image analysis has been an important tool in analyzing and evaluating various geographical and biological images to extract information from them in order to utilize in further study [1]–[6]. In medical sciences, image analysis is used to elaborate the various images taken from internal and external body parts to be used in diagnosis and treatment of diseases [7]–[9]. In addition, this is extensively used in evaluating the biological images to investigate detailed cellular mechanism relevant to physiological processes and diseases [10], [11]. Mammalian cells interpret chemical signals, such as growth factors, hormones and extracellular matrix (ECM) proteins to respond to external cues. Trans-membrane proteins like receptor tyrosine kinases (RTKs) bind specific growth factor ligands, such as platelet-derived growth factor (PDGF), fibroblast growth factor (FGF), and epidermal growth factor (EGF), and these together activate signaling pathways that regulate cell adhesion, migration, and differentiation in a broad spectrum of cell types. These signal transduction pathways generally involve protein translocation and covalent modifications of signaling molecules. Inappropriate activation of these pathways is a common occurrence in pathological and developmental diseases, including human cancers [10], [12].

Cell migration is a central process in the development and maintenance of multi-cellular organisms. Tissue formation during the embryonic evolution, immune responses and wound healing etc. substantially requires cell migration in a particular manner to a specific zone. A thorough understanding of the driving variables' function in this case would certainly be evocative in developing the basic strategies for controlling the diseased cells [13]. It is

suggested that, a particular type of kinase is one of the main components responsible for cell migration inside our body system. This kinase is known as Phosphoinositide 3-kinase (PI3K). The phosphoinositide 3-kinases (PI3Ks) are a family of proteins involved in the regulation of cell survival, growth, metabolism, and glucose homeostasis where increased PI3K activity is often associated with higher migration behavior as seen in many cancers [14]–[16]. Although the both random and directed cell movement are analyzed extensively in different studies, the exact sophisticated regulation during random migration is yet to be established [12], [15], [17]–[19]. Erik S. Welfet *al.* stated that localization and movement of phosphoinositide 3-kinase (PI3K) signaling is supposedly play an important role in cell motility, yet the regulatory functions of this pathway have not been sufficiently interpreted [11]. Understanding the PI3K-AKT-mammalian target of the rapamycin (mTOR) tumor cell signaling pathway can open the door towards more advanced adapted breast and ovarian cancer therapy as it contributes in the onset and progression of tumor growth, and regulates essential cell functions, including replication, proliferation, and uptake [20], [21]. Moreover, recent findings suggested that this pathway have a significant contribution to gastric cancer [22]. Evidence has been found to confirm the function of the PI3K-AKT-glycogen synthase kinase (GSK3) signaling network of neuronal cells underpinning the production and treatment of psychotic disorders [23]. It is suggested that the polarity in signaling in cell might have direct influence on the preferred direction of cell migration [24], [25]. Some of the studies have claimed that cell migration is carried out by adhesion receptors, such as integrin, that links the cell to extracellular matrix ligands, with forces and signals essential for locomotion [26], [27].

Although some studies sought to explain cell migration and its behavior and speed pattern in context of adhesion and polarization concepts, a conclusive study has yet to be found. Detailed investigation of cell migration pattern and intracellular signaling could reveal some fine detail leading to the diagnostic of severe diseases like cancer. Utilization of image analysis techniques can facilitate this significantly as evident from some earlier studies [2], [4], [7], [11], [28], [29]. There are several available tools for analyzing images, however, most of these tools lacks flexibility, and applicability in varying applications. On the other hand, computational language-based image analysis approach offers the desired flexibilities without the limitations of the commercially available tools. To investigate that further, custom computational language-based codes have been utilized to analyze randomly migrated mammalian cells. The primary focus is to establish the possible relationship between the PI3K activities with the cell migration direction. Findings from this study can contribute to the current knowledge base and further pave the pathway for future exploration.

2. Materials and Methods

2.1 Cell culture

NIH 3T3 mouse fibroblasts (American Type Culture Collection, Rockville, MD) expressing EGFP-AktPH was subcultured using Dulbecco's modified Eagle's medium supplemented with 10% v/v fetal bovine serum and 1% v/v penicillin/streptomycin/glutamate as the growth medium. Glass coverslips were cleaned, sterilized, coated with fibronectin (10 mg/ml) for 1 h at 37°C, washed with deionized, sterile water, and dried within 30 min of the experiment. Cells were serum-starved for 2 h and then detached with a brief trypsin-EDTA treatment and suspended in the imaging buffer (20 mM HEPES, pH 7.4, 125 mM NaCl, 5 mM KCl, 1.5 mM MgCl₂, 1.5 mM CaCl₂, 10 mM glucose, 1% v/v fetal bovine serum, 2 mg/ml fatty-acid-free bovine serum albumin). After centrifugation, the cells were resuspended in imaging buffer and plated on the fibronectin-coated coverslips at a density of 10,000 cells/ml and allowed to spread for 1 h before imaging. Mineral oil was layered on top of the buffer to prevent evaporation during the experiment.

2.2 Imaging

Live cell imaging was performed under a total internal reflection fluorescence (TIRF) microscope where fluorophores within ~ 100 nm of the substrate-cell solution interface were selectively excited [30]–[32]. It illuminates the plasma membrane-substrate contact area of cells and ~5-10% of the cytoplasm directly above in fibroblasts.[14]. A TIRF microscope can detect the PIP3 lipid concentration in the cell membrane which can be better visualized by the pseudo coloring of the images. A high color would mean a high concentration of PIP3 and as it was produced from PI3K protein, it would eventually mean a high activity of PI3K in that particular-colored region.

2.3 Evaluation of image parameters

The customized programs were written in MATLAB (MathWorks, USA) takes sequential images (2-minute interval) as input and evaluate different morphological as well as intensity parameters such as intensity, outline, centerline intensity, area, protruded area, retracted area, centroid, cell perimeter, eccentricity, ratio of protruded area to retracted area and cell velocity. The intensity of an image was calculated as the average of the intensities of all pixels in the image. Borderline intensity data of the images were calculated by creating an intensity band of the cell of a specific measure (10/20 pixel) around its border and centerline intensity was calculated simply by subtracting intensity band image from the original image. The area of all individual objects in the image was calculated by using *regionprops* function.

For protruded and retracted area input images were first segmented using K-means segmentation technique for background subtraction and then a binary mask of original image and segmented image was created. This technique was chosen because it is one of the most widely used algorithms for image analysis and is very suited to data with undefined groups or categories, which is the case with our data of interest. The optimal value of K, which corresponds to the number of clusters within the data, was determined using the trial-and-error method. Finally, that binary mask was multiplied with raw image (background subtracted) and protruded and retracted images were developed. Relevant properties of protruded and retracted images were calculated using *regionprops* function. Eccentricity can be considered as a measure of how much the conic section deviates from being circular. Perimeter and Eccentricity were also calculated using *regionprops* function.

2.4 Cell migration velocity

Cell centroid was calculated using *regionprops* function. Before using *regionprops* very tiny and small objects (mostly noise) were removed using area filtration. From centroid position at different time points, travelled distance and velocity were calculated using general algebraic formula.

If two consecutive centroid values are (X₁, Y₁) and (X₂, Y₂) then,

$$\text{Distance} = \sqrt{(X_2 - X_1)^2 + (Y_2 - Y_1)^2}$$

$$\text{Velocity} = \frac{\text{Distance}}{\text{Time}}; \text{ Here, Time} = 2 \text{ minutes}$$

2.5 Development of the proposed hypothesis

The high intensity regions of the main cells were isolated using k-means segmentation method and then the centroid of all individual high intensity regions were determined. Distance from main cell centroid to all high intensity regions' centroid were calculated and stored for future use. For angle

calculation, a line was drawn between two consecutive main cell centroids. Lines between first cell centroid and centroids of high intensity regions were drawn and angles between first line and second lines were calculated and stored. In Figure 1 'a' and 'b' are the centroid of two consecutive cells. A line between 'a' and 'b' was drawn and lines from 'a' to other high intensity region's centroid were also drawn and angles between line 'a-b' and 'other centroids' were calculated.

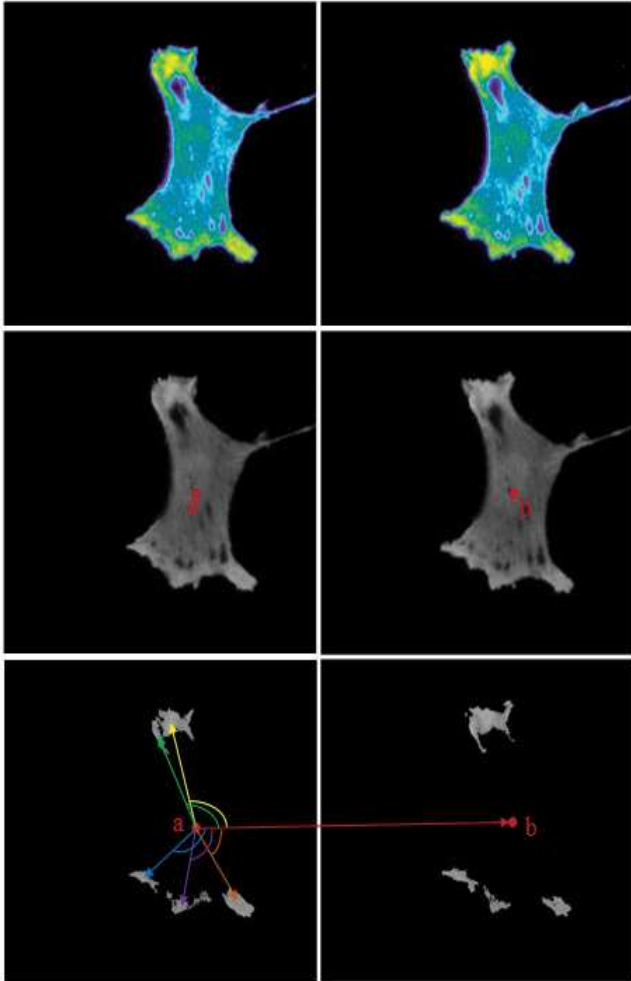


Fig. 1: Angle between two main cell centroid line and high intensity regions' centroids

3. Results and Discussion

3.1 Ratio of protruded area to retracted area

During typical random migration cell tends to move in various directions. In order to map the cell migration to find any directional activity, protrusion and retraction areas are calculated from consecutive images. Protrusion was calculated overlapping one image with the previous one and retraction is the reverse. As seen in Figure 2, the ratio of protruded area to retracted area was found to be between 1.1 - 0.9 and it indicates that the movement speed of the cells along the timeframe is relatively consistent with a slight variation. Moreover, similar area of protruded and retracted region also supports the idea of dynamic equilibrium of the

protein activity inside the cell.

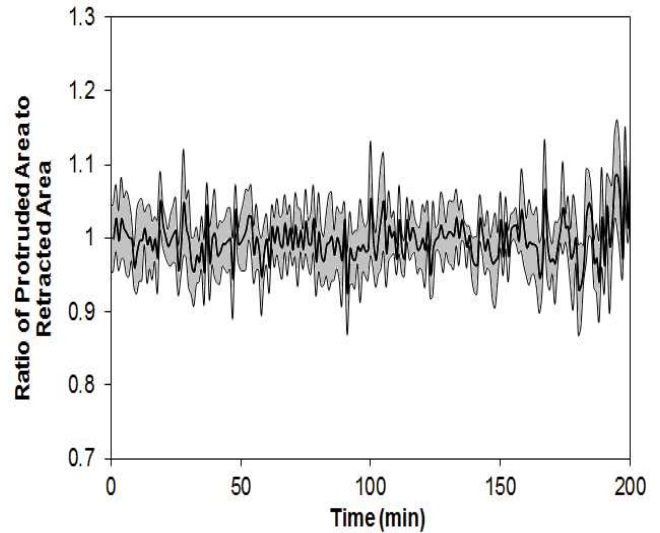


Fig. 2: Ratio of protruded area to retracted area for randomly migrated NIH3T3 Mouse fibroblast cells. Black line represents the mean of 12 different cells and the grey region indicates 95% confidence interval.

3.2 Cell perimeter and eccentricity

Cell perimeter varied from cell to cell and so did the eccentricity (Figure 3), which is a measure of how much the cell adhesion area deviates from being circular. When a cell is highly dynamic, it protrudes in several directions and thus the eccentricity changes with time. High eccentricity indicates the higher level of activity of the cell on the surface. As expected, the cell perimeter increased with the increase in eccentricity for most of the cases. Little deviation from the behavior was also observed at high eccentricity, which is because of elongated morphology of the cells. For slow moving cells, the activity was less and thus the relation between cell perimeter and eccentricity did not very much.

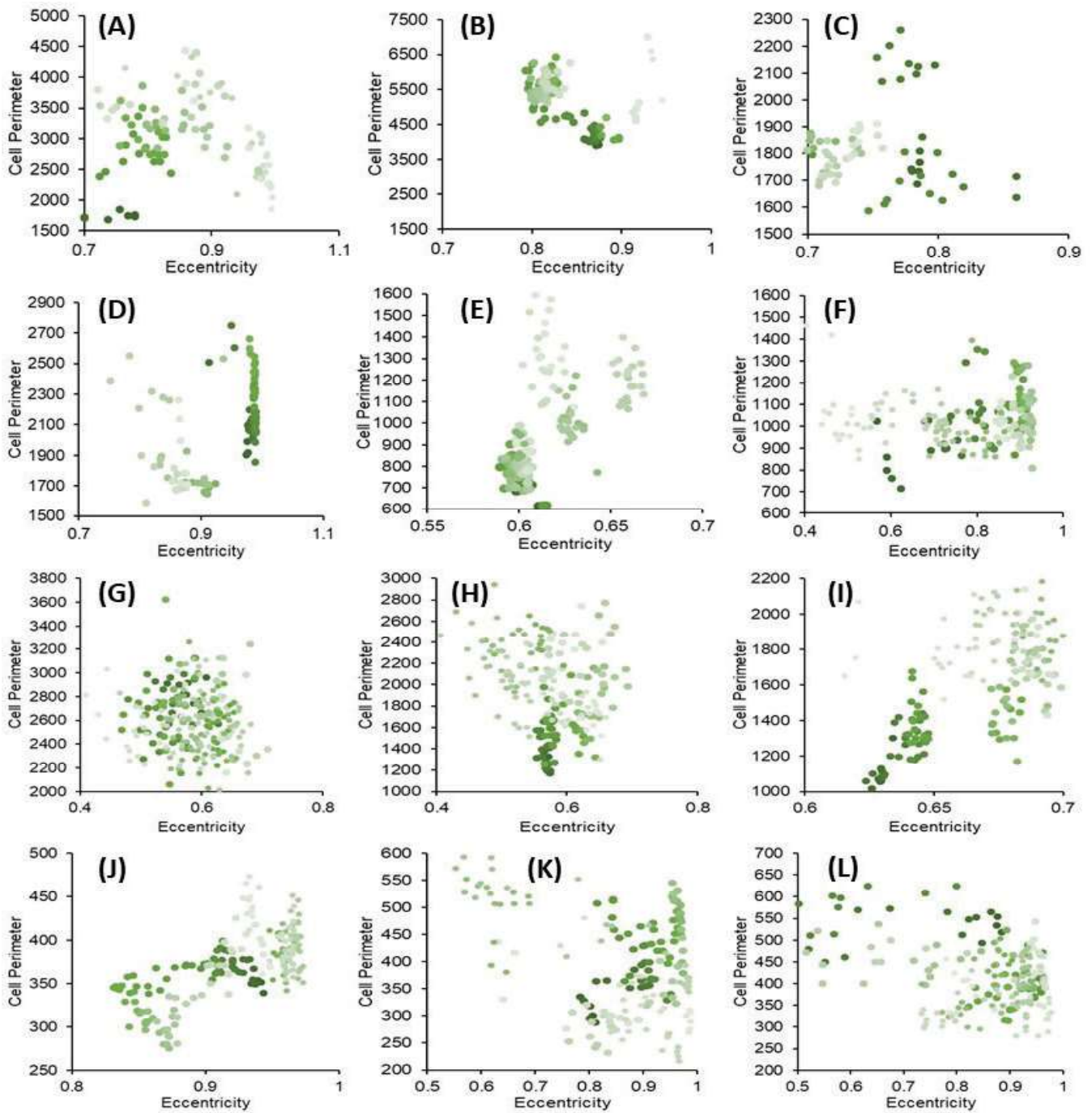


Fig. 3: Change in Cell Perimeter with Eccentricity for NIH 3T3 Mouse fibroblast cell. Color intensity of the data point increase chronologically

3.3 Ratio of cell area to cell perimeter

The area-perimeter ratio of the cells indicates the variations of cellular area and cellular perimeter with the time (Figure 4). When the cell is very dynamic and protrudes significantly, the cell perimeter can be very large despite the cell area being the same. In these cases, this ratio will be lower. The ratio decreases somewhat over time, indicating a relative increase in cellular activity. However, the individual cell migration velocity did not exhibit any significant increase with time (not shown here). On the other hand, cellular eccentricity increased to different extents over the time for individual

cells. This supports the previous relationship of higher eccentricity with higher cellular peripheral activity. It is to be noted that the experiment was not initiated from any standstill condition, rather imaging was started from a random time point. Therefore, the slight increases in activity with time could be attributed to the possible photoactivation of the protein signaling caused during sequential imaging as well as possible photobleaching that might have reduced the intensity slightly causing the reduction of visible cell area [33], [34].

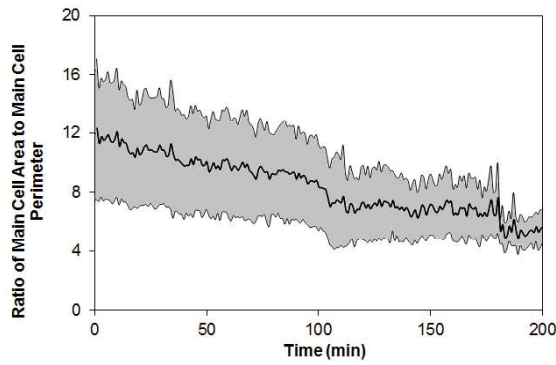


Fig. 4: Change in ratio of cell area to cell perimeter with time for NIH3T3 Mouse fibroblast cell. Black line represents the mean of 12 different cells and the grey region indicates 95% confidence interval.

3.4 Relationship between intensity and velocity

Figure 5 shows the variation of velocity profile with intensity of the main cell and protruded and retracted areas. The main cell velocity did not vary significantly over the time, however, the velocities of the protruded and retracted varied significantly at similar intensities. The plots indicate that the overall cell velocity is not changing significantly despite higher intensity (higher PI3K activity), however, protruded and retracted velocities were higher due to activity of the cellular membrane. In addition, from Figure 6, it was evident that higher velocity was observed exclusively for higher eccentricity, however, lower velocity was observed for varying eccentricity values. This also confirmed that cell migration was essentially controlled by the peripheral activity rather than the overall cell activity [3], [11], [35].

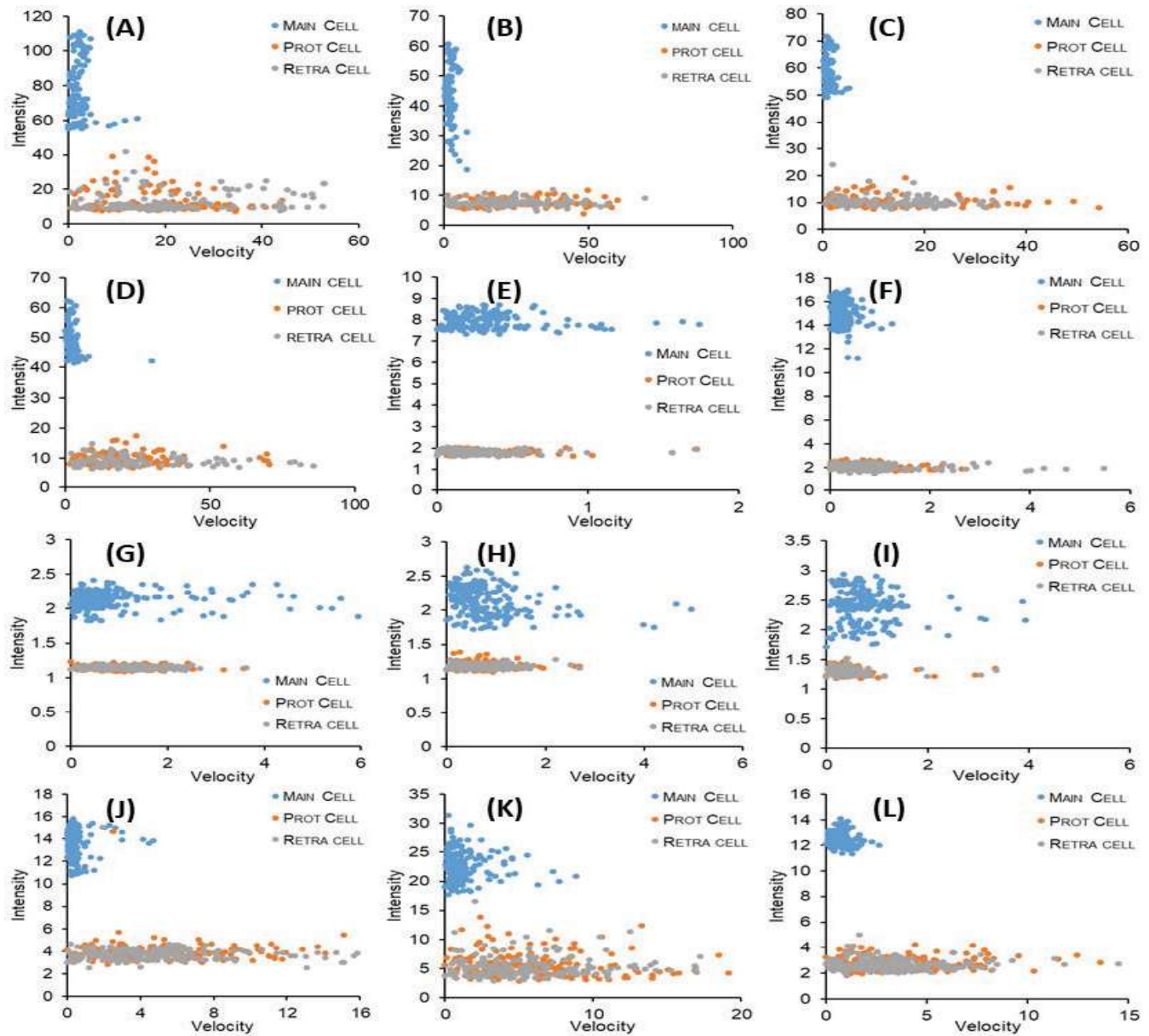


Fig. 5: Change in Intensity with Velocity for NIH3T3 Mouse fibroblast cell, for total cell area, protruded area and retracted area.

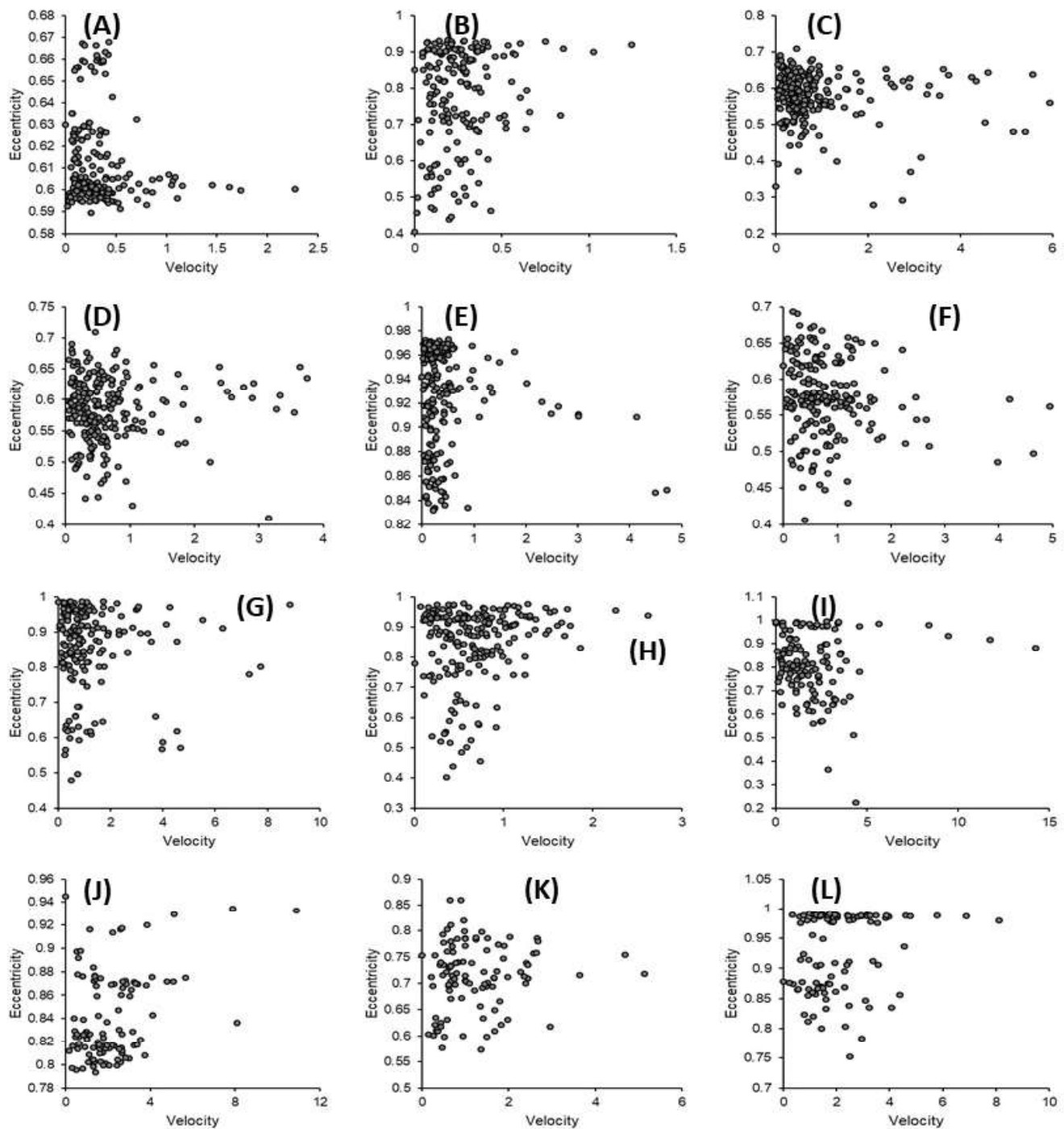


Fig. 6. Change in Eccentricity with Intensity for NIH3T3 Mouse fibroblast cell.

3.5 Relationship between intensity and eccentricity

From the average cell intensity vs. eccentricity plots (Figure 7), a weak correlation of these two parameters was observed. For most of the cells, with the increase in eccentricity, the average cell intensity was either decreasing or remained unchanged. Only few cells exhibited weak positive correlation. This can be explained by the fact that higher eccentricity was caused by higher level of activity at the membrane causing the generation of protrusion and

retraction more frequently. This was mediated by proteins and lipids in different levels. As only bottom membrane of the cell was observed through the TIRF microscope, the otherwise engagement of PI3K might have reduced the level at the visible membrane during cell migration. It also aligns with the earlier finding that higher activity is not controlled by most of the cellular PI3K activity except for the peripheral regions.

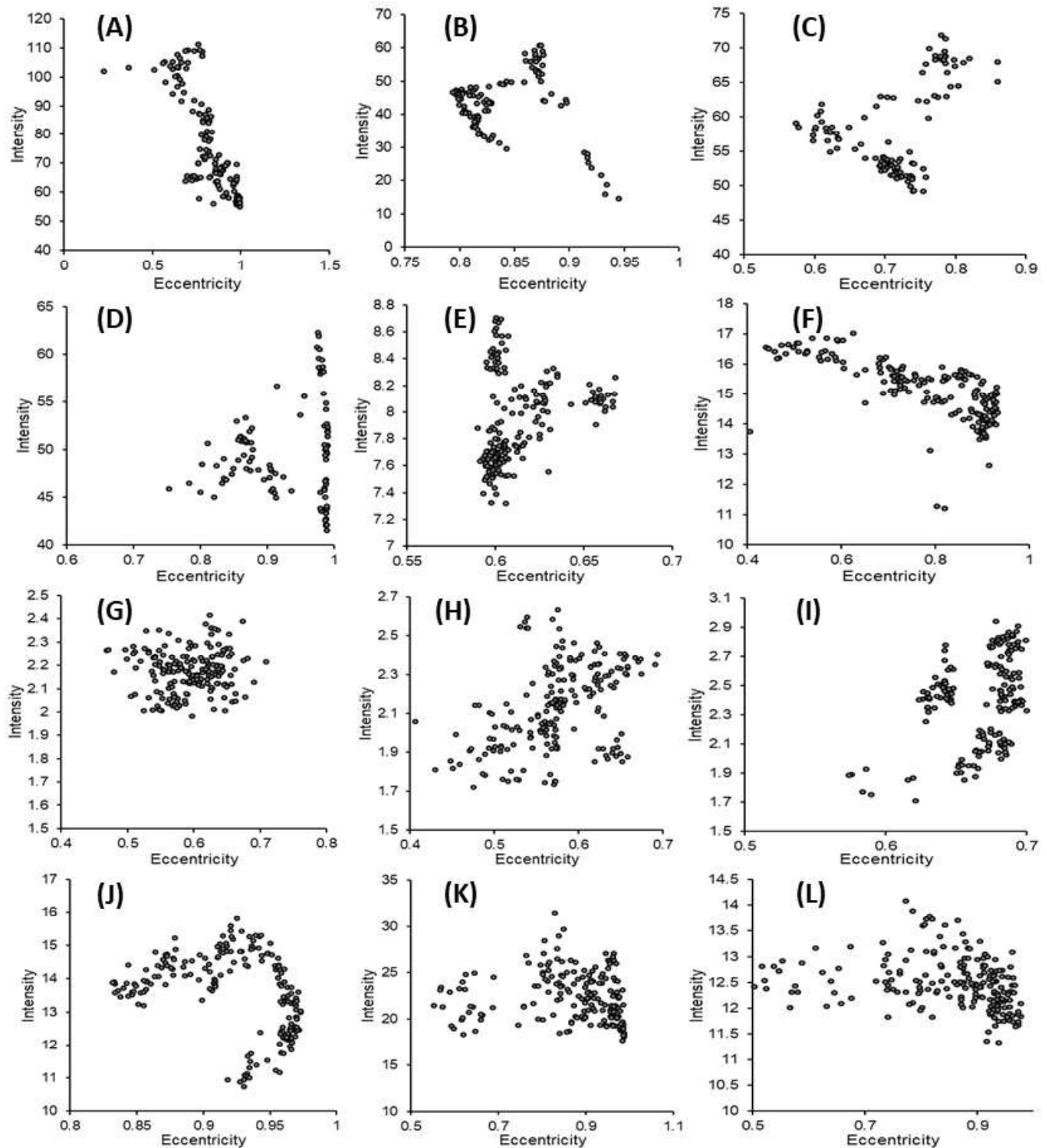


Fig. 7: Change in Intensity with Eccentricity for NIH3T3 Mouse fibroblast cell.

3.6 Evaluation of proposed hypothesis

To explain the preference in cell migration direction and protein interaction in a quantitative way, a parameter named ‘*Signalingstrength*’ has been proposed, which is the contribution made by the intensity and area of a particular high intensity region. This was quantified as a product of these two properties. For each high intensity location, the

ratios of “*Signalingstrengths*” and angles between that region and actual cell migration estimated from the cell centroid were determined (Figure 1).

This ratio can be found for each high intensity regions and is an indication of the force that might play a critical

role in selecting direction during cell migration. Sum of ratio of strength to angle in radian for two lowest angles was calculated and sum of all other ratios were evaluated similarly. Our hypothesis is that two of these ratios will essentially control the cell direction and the cell eventually pick a direction in between these two lines. For example, in case of figure 1 cell direction was determined by the ratios calculated for yellow and orange lines and finally moved to a direction in between these two. In addition, summation

of two ratios corresponding to the two regions with lowest angles were often found larger than the summation of all other existing ratios. As seen from Figure 8, about 85% of cellular data match this hypothesis. This quantitative approach helps to predict the cell migration direction and establishes the crucial role of both the area and intensity of high intensity regions (high level of PI3K activity) in determining cell migration direction.

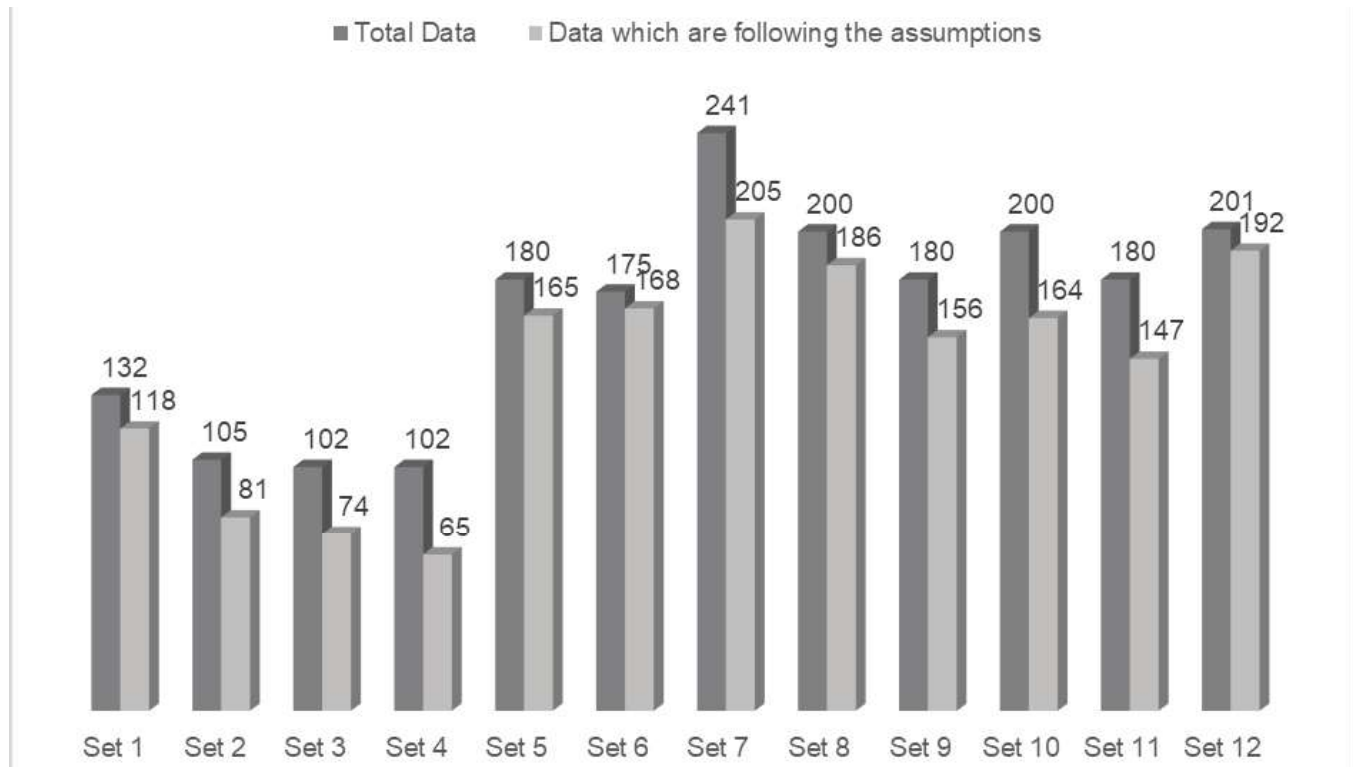


Fig. 8: Comparative scenario of total cellular data and the number of cellular data that followed the proposed signaling strength and angular ratio hypothesis.

4. Conclusions

Cell migration is known to be a crucial factor in a majority of physio-chemical phenomena and therefore, regarded as a crucial criterion in the study of the alteration of the feature in various diseases. However, it has also become evident that cell migration is a very complicated process involving multiple interacting signaling pathways. As PI3K has been identified as one of the primary intracellular proteins involved in this signaling mechanism, hence influencing the migratory behavior of cells, an image analysis strategy has been taken to elucidate this interaction further. In this study, a relation of PI3K protein activity during cell migration has been sought analyzing several sets of biological cellular images using MATLAB based custom coding as an image analysis tool. This study sought to develop a relationship between various parameters based on the activity of PI3K in cell membrane and provides a distinct quantitative linkage between cell migration direction and the high PI3K activity regions in the cell. This study should contribute to the existing knowledge

based on cell migration behavior, which would eventually be effective in disease control and preventive measures.

6. Acknowledgement

The authors gratefully acknowledge the financial support by BUET Chemical Engineering Forum (BCEF) and technical support from Applied Bioengineering Research Incubator (ABRI), BUET during this work.

7. References

1. D. Bong, K. Lai, and A. Joseph, "Automatic Road Network Recognition and Extraction for Urban Planning," *International Science Index, Civil and Environmental Engineering*, vol. 3, no. 5, pp. 205–212, 2009.
2. M. C. Weiger, S. Ahmed, E. S. Welf, and J. M. Haugh, "Directional persistence of cell migration coincides with stability of asymmetric intracellular signaling," *Biophysical Journal*, vol. 98, no. 1, pp. 67–75, 2010, doi: 10.1016/j.bpj.2009.09.051.

3. S. Ahmed *et al.*, "Poly(vinylmethylsiloxane) elastomer networks as functional materials for cell adhesion and migration studies," *Biomacromolecules*, vol. 12, no. 4, pp. 1265–1271, 2011, doi: 10.1021/bm101549y.
4. K. K. L. Wong, Z. Sun, J. Tu, S. G. Worthley, J. Mazumdar, and D. Abbott, "Medical image diagnostics based on computer-aided flow analysis using magnetic resonance images," *Computerized Medical Imaging and Graphics*, vol. 36, no. 7, pp. 527–541, 2012, doi: 10.1016/j.compmedimag.2012.04.003.
5. M. Waseem Khan, "A Survey: Image Segmentation Techniques," *International Journal of Future Computer and Communication*, vol. 3, no. 2, pp. 89–93, 2014, doi: 10.7763/ijfcc.2014.v3.274.
6. T. Ahmed, M. S. Munir, and S. Ahmed, "Segmentation-based Image Analysis Tool for Surveying and Statistical Applications," *International Journal of Signal Processing, Image Processing and Pattern Recognition*, vol. 11, no. 2, pp. 25–32, 2018, doi: 10.14257/ijsp.2018.11.2.03.
7. J. Rittscher, "Characterization of biological processes through automated image analysis," *Annual Review of Biomedical Engineering*, vol. 12, no. 1, pp. 315–344, 2010, doi: 10.1146/annurev-bioeng-070909-105235.
8. N. Sharma *et al.*, "Automated medical image segmentation techniques," *Journal of Medical Physics*, vol. 35, no. 1, pp. 3–14, 2010, doi: 10.4103/0971-6203.58777.
9. F. P. M. Oliveira and J. M. R. S. Tavares, "Medical image registration: A review," *Computer Methods in Biomechanics and Biomedical Engineering*, vol. 17, no. 2, pp. 73–93, 2014, doi: 10.1080/10255842.2012.670855.
10. L. Thomas, H. R. Byers, J. Vink, and I. Stamenkovic, "CD44H regulates tumor cell migration on hyaluronate-coated substrate," *Journal of Cell Biology*, vol. 118, no. 4, pp. 971–977, 1992, doi: 10.1083/jcb.118.4.971.
11. E. S. Welf, S. Ahmed, H. E. Johnson, A. T. Melvin, and J. M. Haugh, "Migrating fibroblasts reorient directionality: By a metastable, PI3K-dependent mechanism," *Journal of Cell Biology*, vol. 197, no. 1, pp. 105–114, 2012, doi: 10.1083/jcb.201108152.
12. R. T. Böttcher and C. Niehrs, "Fibroblast growth factor signaling during early vertebrate development," *Endocrine Reviews*, vol. 26, no. 1, pp. 63–77, 2005, doi: 10.1210/er.2003-0040.
13. C. Migration *et al.*, "Migration 101 - An Introduction to Cell Migration," 2014. <http://www.cellmigration.org/science/>
14. I. C. Schneider and J. M. Haugh, "Spatial Analysis of 3' Phosphoinositide Signaling in Living Fibroblasts: II. Parameter Estimates for Individual Cells from Experiments," *Biophysical Journal*, vol. 86, no. 1 I, pp. 599–608, 2004, doi: 10.1016/S0006-3495(04)74138-7.
15. A. T. Sasaki and R. A. Firtel, "Regulation of chemotaxis by the orchestrated activation of Ras, PI3K, and TOR," *European Journal of Cell Biology*, vol. 85, no. 9–10, pp. 873–895, 2006, doi: 10.1016/j.ejcb.2006.04.007.
16. T. Brock, "The PI3K Pathway: Fast Forward for Cancer," 2009. <https://www.caymanchem.com/news/the-pi3k-pathway-fast-forward-for-cancer>
17. S. A. Eccles, "Parallels in invasion and angiogenesis provide pivotal points for therapeutic intervention," *International Journal of Developmental Biology*, vol. 48, no. 5–6, pp. 583–598, 2004, doi: 10.1387/ijdb.041820se.
18. P. Martin and S. M. Parkhurst, "Parallels between tissue repair and embryo morphogenesis," *Development*, vol. 131, no. 13, pp. 3021–3034, 2004, doi: 10.1242/dev.01253.
19. R. J. Petrie, A. D. Doyle, and K. M. Yamada, "Random versus directionally persistent cell migration," *Nature Reviews Molecular Cell Biology*, vol. 10, no. 8, pp. 538–549, 2009, doi: 10.1038/nrm2729.
20. N. Dey, P. De, and B. Leyland-Jones, "PI3K-AKT-mTOR inhibitors in breast cancers: From tumor cell signaling to clinical trials," *Pharmacology and Therapeutics*, vol. 175, pp. 91–106, 2017, doi: 10.1016/j.pharmthera.2017.02.037.
21. M. K. Ediriweera, K. H. Tennekoon, and S. R. Samarakoon, "Role of the PI3K/AKT/mTOR signaling pathway in ovarian cancer: Biological and therapeutic significance," *Seminars in Cancer Biology*, vol. 59, pp. 147–160, 2019, doi: 10.1016/j.semcancer.2019.05.012.
22. E.-J. Jung, J. H. Suh, W. H. Kim, and H. S. Kim, "Clinical significance of PI3K/Akt/mTOR signaling in gastric carcinoma," *International journal of clinical and experimental pathology*, vol. 13, no. 5, pp. 995–1007, 2020.
23. S. Matsuda, Y. Ikeda, M. Murakami, Y. Nakagawa, A. Tsuji, and Y. Kitagishi, "Roles of PI3K/AKT/GSK3 Pathway Involved in Psychiatric Illnesses," *Diseases*, vol. 7, no. 1. p. 22, 2019. doi: 10.3390/diseases7010022.
24. A. Huttenlocher, "Cell polarization mechanisms during directed cell migration," *Nature Cell Biology*, vol. 7, no. 4, pp. 336–337, 2005, doi: 10.1038/ncb0405-336.
25. V. Kölsch, P. G. Charest, and R. A. Firtel, "The regulation of cell motility and chemotaxis by phospholipid signaling," *Journal of Cell Science*, vol. 121, no. 5, pp. 551–559, 2008, doi: 10.1242/jcs.023333.
26. S. P. Palecek, J. C. Loftust, M. H. Ginsberg, D. A. Lauffenburger, and A. F. Horwitz, "Integrin-ligand binding properties govern cell migration speed through cell-substratum adhesiveness," *Nature*, vol. 385, no. 6616, pp. 537–540, 1997, doi: 10.1038/385537a0.
27. S. L. Gupton and C. M. Waterman-Storer, "Spatiotemporal Feedback between Actomyosin and Focal-Adhesion Systems Optimizes Rapid Cell Migration," *Cell*, vol. 125, no. 7, pp. 1361–1374, 2006, doi: 10.1016/j.cell.2006.05.029.
28. T. Söllradl, K. Chabot, U. Fröhlich, M. Canva, P. G. Charette, and M. Grandbois, "Monitoring individual cell-signaling activity using combined metal-clad waveguide and surface-enhanced fluorescence imaging," *Analyst*, vol. 143, no. 22, pp. 5559–5567, 2018, doi: 10.1039/c8an00911b.
29. Q. Ni, S. Mehta, and J. Zhang, "Live-cell imaging of cell signaling using genetically encoded fluorescent reporters," *FEBS Journal*, vol. 285, no. 2, pp. 203–219, 2018, doi: 10.1111/febs.14134.
30. D. Axelrod, N. L. Thompson, and T. P. Burghardt, "Total internal reflection fluorescent microscopy," *Journal of Microscopy*, vol. 129, no. 1, pp. 19–28, 1983, doi: 10.1111/j.1365-2818.1983.tb04158.x.

31. D. Axelrod, "Total internal reflection fluorescence microscopy in cell biology," *Traffic*, vol. 2, no. 11, pp. 764–774, 2001, doi: 10.1034/j.1600-0854.2001.21104.x.
32. J. A. Steyer and W. Almers, "A real-time view of life within 100 NM of the plasma membrane," *Nature Reviews Molecular Cell Biology*, vol. 2, no. 4, pp. 268–275, 2001, doi: 10.1038/35067069.
33. N. C. Shaner, P. A. Steinbach, and R. Y. Tsien, "A guide to choosing fluorescent proteins," *Nature Methods*, vol. 2, no. 12, pp. 905–909, 2005, doi: 10.1038/nmeth819.
34. N. C. Shaner, G. H. Patterson, and M. W. Davidson, "Advances in fluorescent protein technology," *Journal of Cell Science*, vol. 120, no. 24, pp. 4247–4260, 2007, doi: 10.1242/jcs.005801.
35. A. R. Houket *al.*, "Membrane tension maintains cell polarity by confining signals to the leading edge during neutrophil migration," *Cell*, vol. 148, no. 1–2, pp. 175–188, 2012, doi: 10.1016/j.cell.2011.10.050.